Contract No:

This document was prepared in conjunction with work accomplished under Contract No. DE-AC09-08SR22470 with the U.S. Department of Energy (DOE) Office of Environmental Management (EM).

Disclaimer:

Hydride Effects on Discharged Fuel Clad Related to Accident Conditions During Dry Storage and Handling.

R.L. Kesterson, P.S. Korinko, P.S Lam, R.L. Sindelar,

Savannah River National Laboratory. Aiken SC

Keywords: Hydrides, Hydrogen, FEA, Mechanical Testing, Ductile-Brittle Testing, Spent Fuel Clad

For publication in an ASTM STP for the proceedings of the 18th Symposium on Zirconium in the Nuclear Industry, May 15-19, 2016,
Hilton Head, SC, USA

ABSTRACT

Safe handling of nuclear reactor discharged fuel requires an understanding of how the fuel (cladding) will perform under the various encountered conditions, including off-normal events such as drop events in handling the storage canister. Clad failures under two distinct loading modes are considered; a diametrical pinch mode and an axial bend mode. The mechanical response to the pinch mode and the bend mode loading are evaluated with ring compression testing (RCT) and three point bend testing (TPB), respectively. ZIRLO ™ clad samples were hydrogen charged to levels from 100 PPM to 800 PPM and then subjected to a hydride reorientation treatment involving heating to 400^0C and cooling while under hoop stresses ranging from 90 to 170 MPa. Radial hydride reorientations were characterized and RCT and TPB tests were performed over a temperature range of ambient to 200^0 C. Ductile to brittle transition temperatures (DBTT) were determined.

Using finite element analysis (FEA) true stresses and strains are calculated and comparisons made between the RCT and TPB test modes. Due to the anisotropic properties of the clad and the relative orientation and generic effects of the hydrides, the DBTT was observed to be strongly dependent on the mode of strain application such that a DBTT associated with a RCT test is different from a DBTT obtained using an axial bend test. While the degree of radial hydriding strongly affected the pinch mode-RCT test the same radial hydride impact was not observed for the axial bending-TPB test which was strongly impacted by the bulk hydride levels and not the fraction of radial hydrides.

NOMENCLATURE

DBTT – Ductile Brittle Transition Temperature
FEA –Finite Element Analysis
PPM – parts per million by weight also wppm
RCT – Ring Compression Test – Displacement is referred to as the change in diameter with applied load
RHGT – Radial Hydride Growth Treatment (controlled cooling from 400°C to RT while under a preset (initial) hoop stress)
RXA – Recrystallize Annealed
SRA – Stress Relief Anneal
TPB – Three Point Bend – axial bending – Deflection is referred to the distance the tube OD at mid span moves with the applied load.
TSSD – Terminal Solid Solubility - Dissolution
TSSP – Terminal Solid Solubility - Precipitation

INTRODUCTION

Reactor site fuel pools are running out of storage area for the discharged fuel and the most used current alternative is to load the fuel assemblies into containers, remove the residual water (dry), place into casks and store for an interim period at the reactor site. Planning for this storage includes an evaluation of potential accident conditions and designing the systems to perform acceptably. An important factor for the fuel clad is to maintain some degree of ductility when the stored fuel is being moved and is susceptible to a container drop type accident. Hydriding in zirconium cladding along with radiation generated lattice defects cause embrittlement which can be characterized by a ductile-to-brittle transition temperature evaluation. Maintaining the clad temperature above a threshold temperature (DBTT) is one way to enhance the ductility margin. The focus of this program is characterization of the DBTT of hydrided cladding under two different failure modes.

Plausible off-normal accident scenarios in storage, handling, and transport of spent fuel in dry storage systems are drop events. Clad staining under such events would occur, and the response of the cladding and its potential to fail are dependent on the material condition of the cladding, and the loading mode.

A likely canister dry out procedure will include a self-heating of the fuel to temperatures near 400 C. At this temperature about 200 PPM of the clad hydrogen will be in solution. As the clad cools this H will precipitate as hydrides. These hydrides represent potential crack paths and the orientation of these hydrides is dependent on many variables, such as:

- stress orientation,
- temperature differentials,
- pre-existing hydride morphology (memory effect related to lower activation energy to re-precipitate and grow with existing hydrides rather than to nucleate new ones),
- crystallographic orientation,
- grain morphology and microstructure

- alloy composition (including composite structures like duplex or lined cladding).
- cooling rates (not well studied for representative dry storage cooling rates but very slow rates may affect hydride orientations by favoring non-stress mechanisms such as minor temperature differentials and re-precipitation along prior or existing hydrides).

To better understand the response of hydrided cladding to off-normal loading scenarios, testing was performed to evaluate the ductile to brittle transition temperatures for different failure modes. A series of ring compression tests (RCT) and three point bend tests (TPB) were performed to provide a comparison of characteristics related to accident conditions involving fuel rod axial bending (TPB) and fuel rod pinch loading (RCT). The testing reported is on unirradiated material and does not fully duplicate the actual fuel rod cladding condition; however, this characterization testing provides data on the DBTT trends related to hydride levels and morphology with a focus on radial hydrides.

For this series of tests it was assumed that a temperature of 400 C was the peak temperature that the clad would experience during drying. At this temperature the hydrogen solubility is about 200 to 250 PPM. If a section of the cladding has 400 PPM then about 50% of the hydrogen would go into solution and subsequently re-precipitate as hydrides upon cooling. Likewise, if a section of cladding has 200 PPM or less then effectively all of the hydrogen would go into solution and re-precipitate as hydrides upon cooling. This is an important factor to consider since the higher relative amounts of hydrogen in solution versus the hydrogen remaining typically as circumferential hydrides will result in higher ratios of re-precipitated hydrides to existing hydrides. As will be shown in a later section the ratio of radial to circumferential hydrides is a major variable in considering RCT DBTT levels.

Reference **1** provides details on the testing techniques and initial RCT data. This paper provides a summary of the test results and additional information on radial hydride to circumferential hydride ratio effects, FEA analysis, TPB test results, compares TPB to RCT DBTT values, impact of quartz filler pellets in RCT test, and supporting data for the conclusion that the hydrogen related RCT and TPB DBTT values are significantly different.

Clad stress level variations: During dry storage the primary clad stress is in the hoop direction and is a function of the internal gas pressure from fission gas release, initial fill gas and in some designs gas generation from rod internal burnable neutron absorbers. The majority of the internal gas is in the fuel rod plenum(s) which typically will be at lower temperatures than the peak clad temperatures because of their locations near rod ends. A typical peak hoop stress of 90 MPa is used for storage design **[2]**; however, higher internal pressures/hoop stresses are possible for some fuel rod conditions. The actual fuel rod conditions will vary with design and operating duties; thus, initial values of 90 MPa and 130 MPa were chosen to study the effects of hoop stresses on hydride reorientation. To represent an extreme condition, 170 MPa was also included in the test matrix. The hoop stress variable is only applied to the development of radial hydrides and the internal hoop stress is not present during the mechanical testing of the samples.

Ductile to Brittle Transition Temperatures (DBTT): For accident evaluations regarding spent fuel transport, storage, and retrieval it is of value to know the degree of strain that can be accommodated by the clad prior to reaching a point of crack initiation and unstable propagation.

Classically this temperature/material condition has been associated with DBTT. DBTT type tests have been done in the past on cladding, primarily using ring compression testing (RCT) which corresponds to a diameter crush test in an accident drop scenario. In this test series both RCT and TPB testing was performed on sample tubes with similar hydride morphology to generate comparative DBTT characteristics.

Failure Modes

A schematic showing the clad failure modes for a container drop accident is shown in Figure 1 **[3].**There are basically three modes of stress present; Mode I and II are bend modes (lateral deflection between grid support points) represented in this testing by three point bend tests and Mode III which is a pinch or diameter crush mode represented by ring compression testing. For Mode –III the reference source of Figure 1 included a PCI crack as an additional feature but that is not included in these tests. It is proposed that in potential container drop type accidents that strains leading to Modes I and II failures are more probable than strains leading to a Mode-III failure. This proposal is based on two primary reasons: (1) there will be stiff pellet résistance to diameter displacements when pellet-clad contact is made (prior to significant amounts of diameter displacements) and (2) it is postulated that the rod movements during an accident will result in random displacements which will promote axial bending stresses.

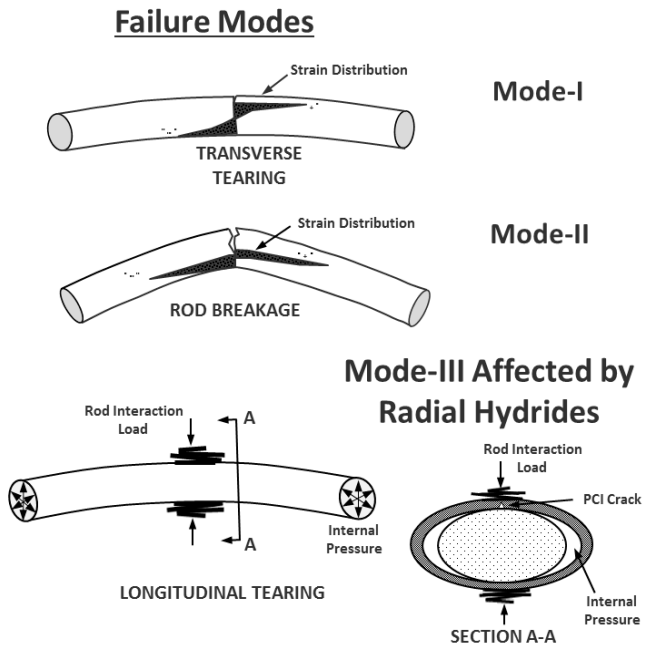

Figure 1- Examples of Three Primary Clad Failure Modes (Adapted from reference 3)

TEST PROCEDURES AND PARAMETERS

Materials

Standard stress relief annealed (SRA) ZIRLO™ tubing was used for this study. The nominal composition of ZIRLO is 1% Sn, 1% Nb, 0.1% Fe, and 0.10-0.14% O. The tube samples had nominal dimensions of 9.52 mm OD and 8.38 mm ID (0.375 inch OD and 0.330 inch ID). Samples were cut to two lengths of 0.8 cm for the ring test and 11.4 cm for the bend test. The initial hydrogen charging was performed on longer tubes (38 cm/15 inches long) from which the test samples were later wire EDM. High purity hydrogen and high purity argon, 99.95% purity, were used to charge and pressurize the ZIRLO tubes, respectively.

Specimen Preparation

Tubing samples were pre-hydrided to target levels of 100 PPM, 200 PPM, 400 PPM and 800 PPM. The area designated for hydrogen charging was lightly abraded on the OD surface using 600 grit silicon carbide paper and cleaned with absolute alcohol. The cleaned and air dried samples were placed in a stainless steel tube furnace and evacuated within 20 minutes of final cleaning, consistent with a process developed for hydrogen charging Zircaloy-4 **[4].** The samples were evacuated for a minimum of 12 hours prior to the introduction of the appropriate aliquot of hydrogen.

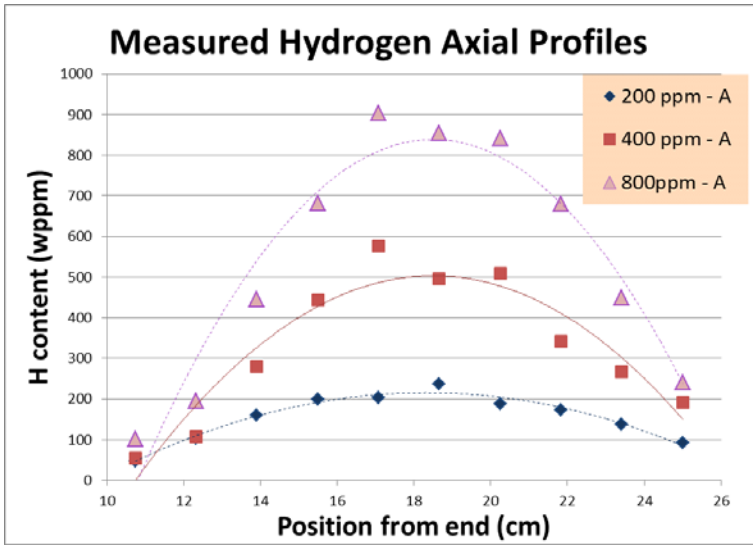

Figure 2- Charged Tubes Hydrogen Profiles

During hydrogen charging the furnace tube was heated to 400°C at a rate of 10°C/min, held for 30 minutes, and then cooled at a rate of 5C/min to 100°C and allowed to convectively cool to RT. Rings from the charged tube were evaluated for hydrogen content using a LECO Hydrogen Gas Analyzer. Variation in hydrogen content was observed along the tube axis as shown in Figure 2. The measured axial hydrogen level varied more in the higher hydrogen content samples

than in the 200 PPM sample. Specific hydrogen levels were not measured on individual RCT or TPB samples. The calculated hydrogen loading was assumed to be representative of the sample condition. This does introduce some uncertainty; however, the hydrogen loading aims have relatively large incremental differences in hydrogen levels and the trends showing the effects of increasing hydrogen levels should not be significantly affected by small variations in the absolute hydrogen levels in the samples. The available hydride microstructure information indicates a generally distributed circumferential hydride structure across the sample wall for the 100, 200 and 400 PPM samples viewed. This is expected since there was no high temperature hydrogen homogenization treatment performed.

The ring test samples were cut from the mid-section of the charged tubes where the hydrogen levels were most consistent. The bend test samples were also cut from the center of the charged and aged tubes and the stress- strain maximums during the bend tests are concentrated near the sample mid length at the position of contact with the upper roller.

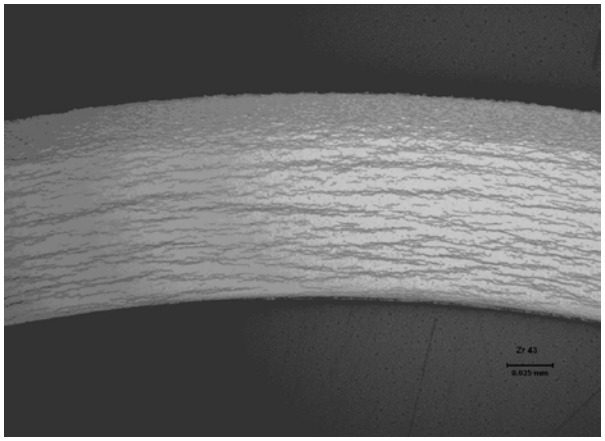

Figure 3A- Example of 800 PPM charged Sample with OD rim

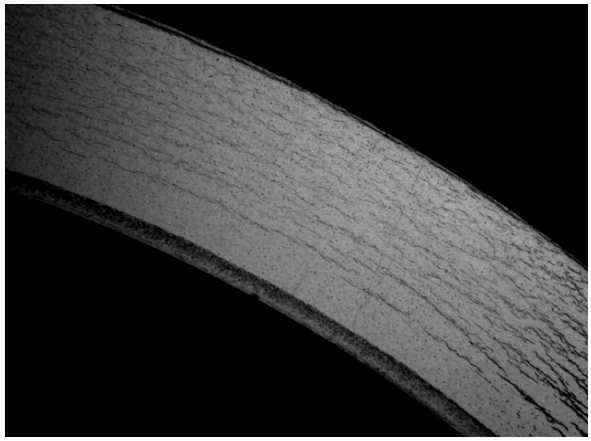

Figure 3B- Example of 800 PPM charged Sample with ID rim

Depending on the specific hydrogen charging procedure an ID or OD hydride rim was observed for the samples with nominally 800 PPM hydrogen. Examples are shown in Figures 3A and 3B. Also on a few of the 400 PPM samples there was a relatively small hydride rim observed.

Radial Hydride Growth Treatment (RHGT)

One objective of this evaluation was to measure the effects of hoop stress on hydrogen reorientation during cooling. Pre-hydrided samples were pressurized with Argon to achieve the desired stress for the RHGT; higher pressures than indicated by Boyles' law were needed since the entire system volume was not heated, however, the system pressure was monitored to ensure the initial pressure was adequate to achieve the desired RHGT pressure. The resultant hoop stress is calculated as:

Hoop stress = pressure x (ID+OD)/2 / wall.

The sample was inserted into the furnace and the furnace was heated to 400°C at a rate of 10°C/min, held for one hour, and cooled at a rate of 5°C/hr to 200°C and then air cooled to room temperature. During cooling the hoop stress also decreased with decreasing temperature. This method produces a peak hoop stress that decreases with decreasing temperature. This is an important factor to consider when determining threshold stress levels for radial hydride reorientation. With the thermal hysteresis between TSSD and TSSP there is an incremental amount of cooling that occurs prior to the start of hydride precipitation. This temperature drop produces a pressure / hoop stress decrease from the initial value. Also there are further reductions in the hoop stress as cooling continues and additional hydrides precipitate. Thus, the actual hoop stress associated with onset of hydride reorientation will be lower than the peak stress for systems which allow pressure to reduce with cooling.

Following the RHGT radial hydride formation was observed in samples exposed to 130 MPa and 170 MPa hoop stresses. No significant radial hydrides were observed in the 90 MPa stressed samples. An example of this is shown in Figure 4 where increasing radial hydride density is associated with the increasing hoop stress.

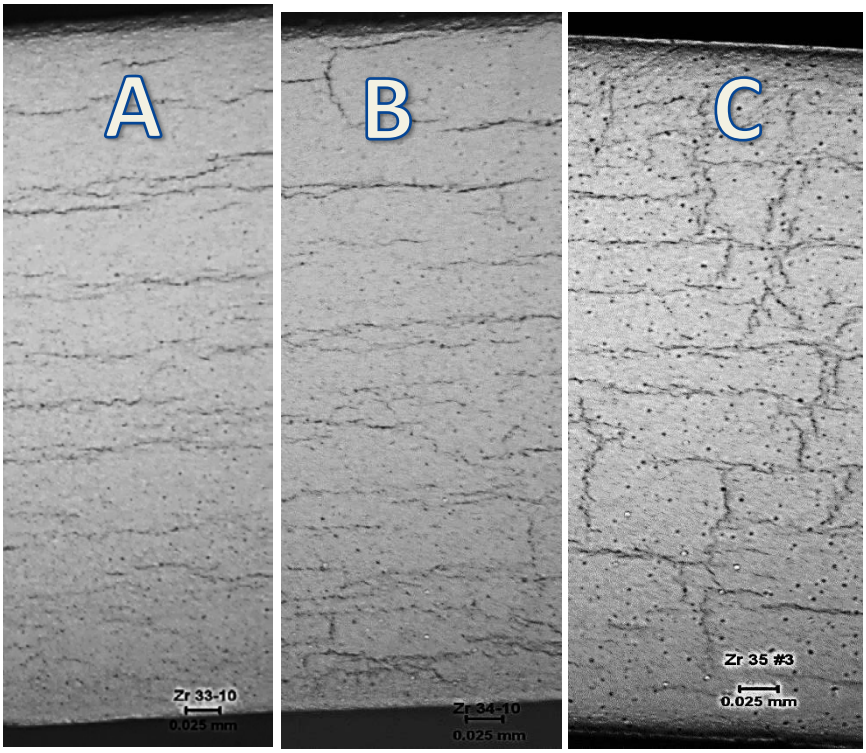

Figure 4- ZIRLO sample charged with 200 ppm H (a) RHGT 90 MPa, (b) RHGT 130 MPa and (c) RHGT 170 MPa

Examples of typical hydride microstructures observed after RGHT (with cooling from 400^0 C to 200^0 C at 5C/hr) are shown in Figures 5A, 5B and 5C. The 200 PPM and 400 PPM samples look like they

may have similar hydride distributions but this effect is attributed to variations in degrees of hydride etching and that the 400 PPM samples has a small hydride rim forming on the ID. The 800 PPM sample has an ID rim where a portion of the hydrides are concentrated. Also for the 800 PPM sample it appears that the rim formation/growth has scavenged some of the inner wall hydrides and left a semi-denuded hydride zone. For the 800 PPM samples with significant hydride rims there is an expected effect on the crack initiation strain dependent on the rim position relative to the maximum strain position. The RCT and TPB ductilities are consistent within the 800 PPM data sets and suggest that the ID-OD rim position is not a large variable and does not significantly impact the trend comparisons between the 800 PPM samples and the 100, 200, and 400 PPM samples.

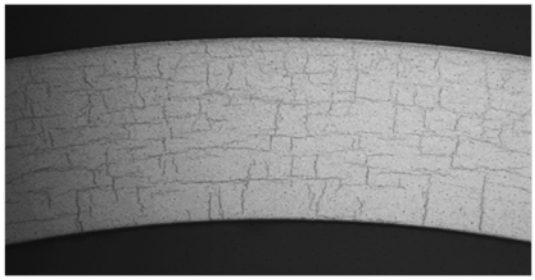

Figure 5A-100 PPM, 170 MPA

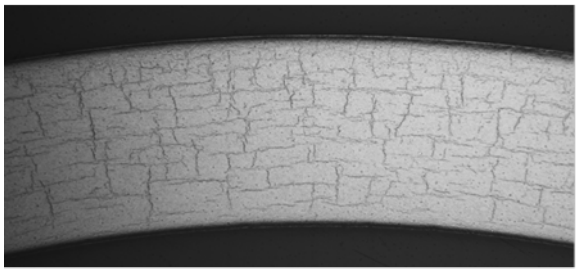

Figure 5B-200 PPM, 170 MPA

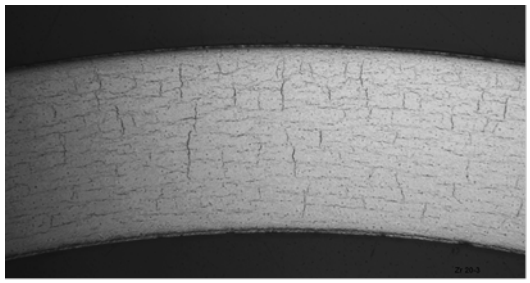

Figure 5C-400 PPM, 170 MPA

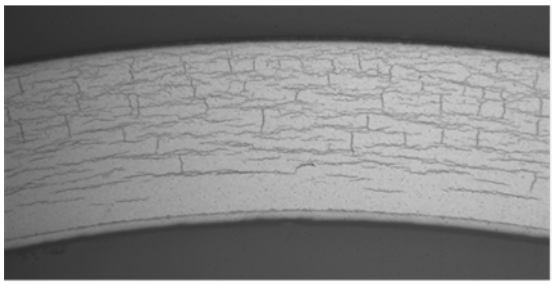

Figure 5D-800 PPM, 170 MPA

The tested material was in the SRA condition and had an axially elongated grain structure. If the tube was in a RXA condition with large equiaxed grains there would be a tendency for longer radial hydride formation. Figure 5 shows most radial hydride growth terminating when intersecting existing circumferential hydrides.

For the RCT samples the major tensile stress is a hoop or circumferential stress. This stress direction is normal to the radial hydride platelets which tend to have a radial – axial orientation. The resulting crack propagation from RCT tests runs parallel to the radial hydride plane and is postulated to be the reason why RCT tests are very sensitive to the relative radial hydride morphology. For example the RCT crack plane will be in a plane normal to the surface shown in

Figure 5 and running from the OD (or in some cases starting at the ID) to the opposite side. The major tensile stress in the TPB samples is axial and promotes crack growth at a direction perpendicular to the radial hydride planes. The TPB crack plane will be parallel the surface shown in Figure 5. It is postulated that this difference in crack plane orientations in reference to the radial and circumferential hydride planes is a major reason for the observed differences in hydride related RCT and TPB DBTT that are observed in this program.

Ring Compression Testing and Three Point Bend Tests

Mechanical properties were determined using TPB and RCT. Both the TPB and RCT were conducted at constant crosshead speeds of 5 mm/s. The crosshead speed was close to the maximum that the load frame was capable of achieving and similar to the crosshead speed reported for most of the RCT testing done at ANL **[5].**

The RCT samples were Wire Electrical Discharge Machined EDM to 8 mm in length. The mechanical compressions where programed for a diametrical displacement of 1.7 mm initially to correspond to previous displacements used by other organizations**[5]** but the displacement was increased to 2.2 mm to increase the ring strains and obtain data regarding failure points with larger displacement. The RCT and TPB test set ups can be seen in Figures 6A and 6B.

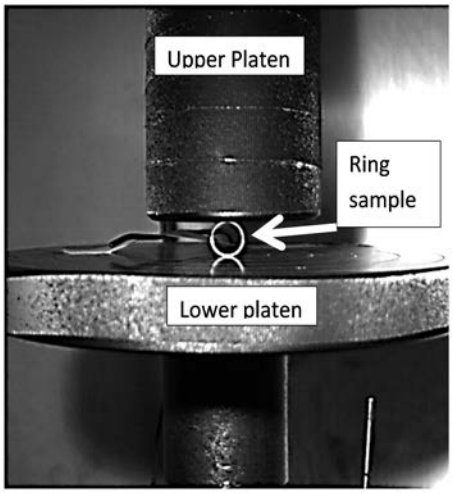

Figure 6A - Ring Compression Test – RCT

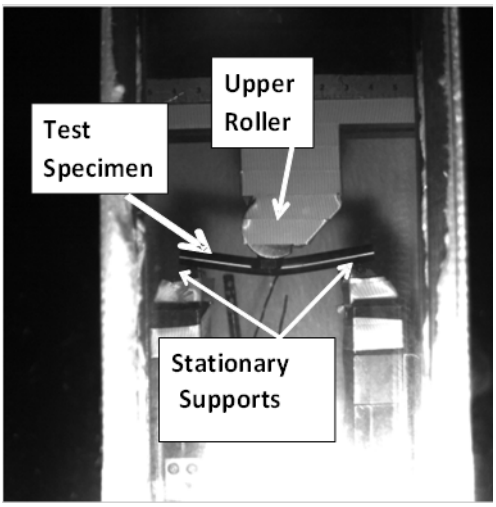

Figure 6B - Three Point Bend Test Fixture

The TPB tests used a span of 92 mm. The stationary supports were 3 mm diameter and the upper roller was 32 mm diameter. Preliminary efforts revealed that the tube had to be filled to avoid buckling (crinkling) and to more closely represent a loaded fuel rod condition. Quartz pellets 8 mm in diameter were cut to 12 mm lengths and loaded into the 8.38 mm ID tube. The tube ends and the quartz pellets were unconstrained. The use of the quartz pellets does not fully replicate the pellet constraints and pellet to clad bonding impacts in actual fuel rods but is an improvement over an open tube test. Initially the bend tests were set for a peak deflection of 6.35mm. Later

tests were taken to larger deflections in order to produce unstable crack propagation in the bend samples.

The ring and bend DBTT testing was performed at temperatures ranging from room temperature to 200°C. This range encompasses cladding temperatures predicted to exist after initial fuel cooldown and at the time of handling and transport after interim long term storage. Temperatures of clad immediately after dry out and initial transport to storage are expected to be higher due to the relatively short cooldown time.

RCT Studies

The initial results from RCT testing have been reported in reference **1**. The following provides information on those initial results to provide a context for the current evaluations.

Typical sets of RCT curves for samples charged with 400 PPM H and with RGHT at 130 and 170 MPa are shown in Figures 7 and 8 respectively. On the curves the areas of plastic yielding are seen when the curve deviates from the linear slope. An abrupt drop in the load is seen during displacement and is assumed to be associated with crack initiation/propagation. The plastic displacement at the initial load drop is used to determine the failure strain for the specific test condition.

The main difference in the samples from these two figures is the RHGT hoop stress levels. Figure 7 has a 130 MPa hoop stress and; thus, would be expected to have lower levels of radial hydrides compared to Figure 8 which represents 170 MPa RHGT hoop stress. It is observed that there are more radial hydrides associated with the higher hoop stress and this higher radial hydride density (or ratio of radial to circumferential hydrides) results in a less ductile structure for RCT testing. Thus, the higher level of radial hydriding (170 MPa samples) results in crack generation at lower displacements than the 130 MPa samples for the same test temperature. When the test data is combined the result is that the 170 MPa samples have a higher DBTT compared to the 130 MPa samples as shown in Figures 9-11.

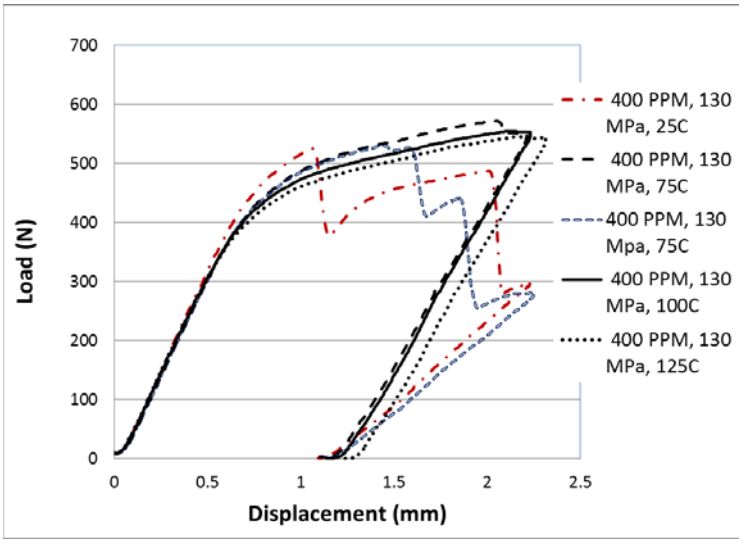

Figure 7 - Example of RCT tests for 400 PPM, 130 MPa RHGT

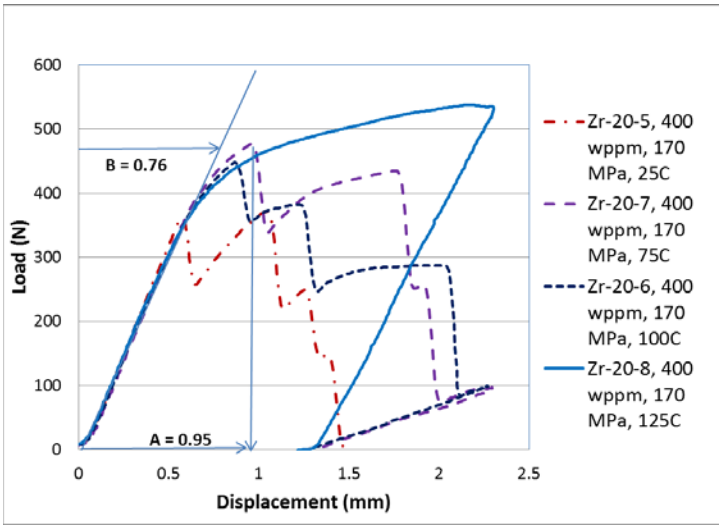

Figure 8 - Example of RCT Charts for 400 PPM, 170 MPa

The RCT samples were tested to a displacement of 1.7 mm and the strain was calculated by dividing the displacement by the nominal diameter. The mechanical strain in the RCT tests is calculated as the percentage of the plastic displacement at failure / sample OD. Using the Zr-20-7 curve from Figure 8 as an example:

Measured total displacement at first load drop = A = 0.95 mm

Extrapolated offset (elastic) strain at load drop = B = 0.76 mm

Sample OD = 9.5 mm

% plastic offset strain = (total displacement – offset strain)/ sample OD

= (0.95 – 0.76)/9.5 x 100 = 2%

% total strain at failure = A/OD x100 = 0.95/9.5 x100 = 10%

Thus this sample is classified as having 2 % plastic / 10% total strain at failure. This is not the true strain but a relative displacement measurement. For these calculations the elastic portion was assumed to be directly related to the loading modulus and not the unloading modulus. The unloading modulus for RCT samples is lower than the loading modulus. This is an effect of the ring sample acting as a mechanical spring and some setting occurring during plastic displacement. The use of the loading modulus to calculate the elastic strain reflects well the stain conditions that would be encountered during accident loading conditions and provides a

consistent basis for relative comparisons. Using the above technique the failure strains as a function of test temperature are shown in Figures 9 through Figure 11.

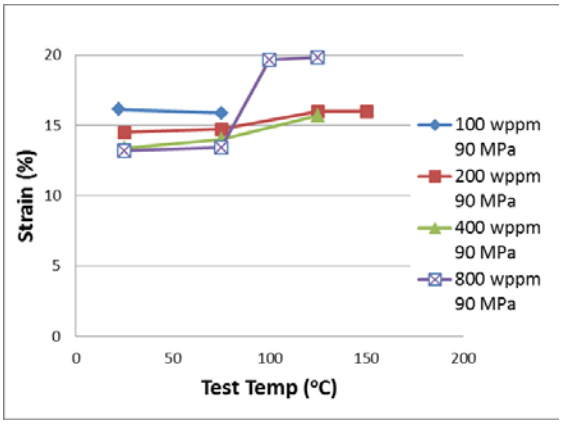

Figure 9- RCT DBTT at 90 MPA

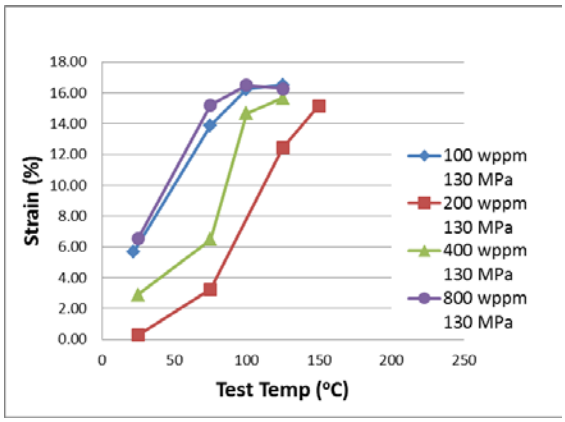

Figure 10 - RCT DBTT at 130 MPa

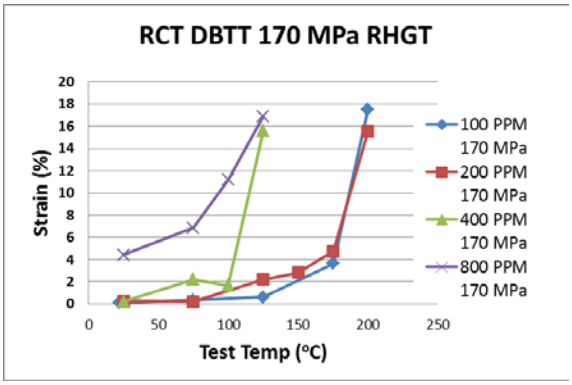

Figure 11- RCT DBTT at 130 MPa

The effects of increasing hoop stress is seen as moving the knee of the curves to higher temperatures; thus increasing the DBTT temperatures. This is not in a desirable direction and is the result of higher hoop stresses producing more radially oriented hydrides with the cooling re-precipitation. At 90 MPa all of the hydrogen levels have a DBTT that is less than room temperature. In these samples the hoop stress was relatively low and no significant radial hydride formation was observed.

The trend for higher DBTT values (lower ductility) associated with lower hydrogen levels is observed and appears counter to the general mechanical property observations of increased ductility with lower hydrogen levels. This trend can be understood from the perspective that hydride radial orientation and not total hydrides is the critical factor for DBTT in the RCT - diameter pinch failure mode. For example the samples with hydrogen levels at 200 PPM would have effectively all of the hydrogen in solution at the RHGT temperature of 400^0C and upon cooling under the higher hoop stresses formed a large portion of radial hydrides which contribute to elevated RCT DBTT results. In the high hydrogen samples of 400 and 600 PPM

there was a large portion of the hydrides that remained as circumferential hydrides during the RGHT and did not re-orient and thus did not contribute to a decrease in ductility.

An anomaly to the postulation that low hydride levels result in higher DBTT is seen in Figure 9 where the 100 PPM sample has a lower DBTT than either the 200 or 400 PPM samples. For this test series it is suggested that:

- The low total hydrogen level results in a longer cool down to reach the lower precipitation temperature relative to the samples with hydrogen levels of 200 PPM and higher.
- The hoop stress strongly affects the degree of radial hydride re-orientation and the hoop stress is related to the temperature. For the 100 PPM sample it is proposed that the hoop stress decreased, due to the temperature reduction, to a level such that there was little radial hydride formation as shown in Figure 12.

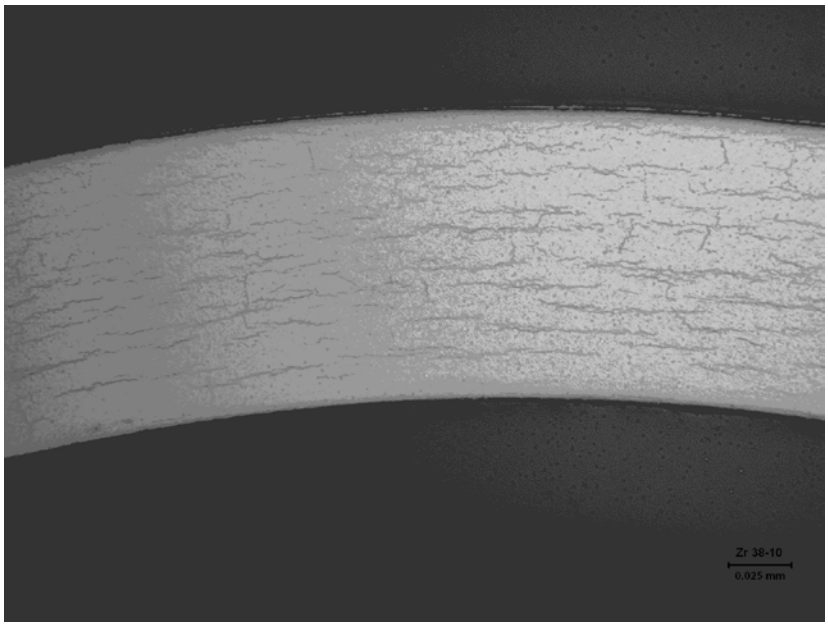

Figure 12- Microstructure of Sample with 100 PPM Hydrogen and 130 MPa RHGT Hoop Stress

Assuming a strain below 2-4% as being in the brittle area, the transition temperature point was interpolated for each hydrogen level and RHGT combination. The choice of 4% in this specific case is based on the temperature and ductility profiles that show a knee at about 4%. To reiterate, the strain % is not the true strain in the material but rather a relative strain. The estimated DBTT values for the different RGHT are listed in Table 1. The lowest test temperature was room temperature or 24^0C. Many samples were observed to be ductile at room temperature and the DBTT classifications are listed as <RT.

Table 1 Ring Compression Tests DBTT			
	RGHT Nominal Pressure (MPA)		
RHGT Hydrogen Level (PPM)	90	130	170
100	<RT	<RT	180^0C
200	<RT	75^0C	180^0C
400	<RT	50^0C	110^0C
800	<RT	<RT	35^0C

Three Point Bend testing

A limited series of three point bend (TPB) tests were performed over a range of hydrogen levels and RHGT hoop stresses as shown in Table 2. The initial test set had samples with 800 ppm that were exposed to relatively low hoop stresses and resulted in few if any radial hydride formation. Two samples with nominally 200 PPM and 400 PPM hydrogen were subjected to hoop – RHGT stresses of 130 MPa and 170 MPA respectively to generate a large fraction of radial hydrides in the microstructure. An additional test was performed on an as-received (un-hydrided) tube to evaluate the bending characteristics without hydrides present. For this series of tests the 200 PPM and 400 PPM samples were tested at room temperature. The 800 PPM samples were tested at room temperature, 75^0 C, 125^0 C, 150^0 C, and 175^0 C to determine a DBTT curve.

Prior to the TPB test the samples were filled with quartz pellets to simulate the resistance of fuel pellets to clad crinkling or buckling which occurs in hollow tube bends. The quartz pellets were 0.38 mm smaller in diameter than the tube ID and so some deformation occurred before contacting the internal quartz pellets. The 800 PPM hydrogen charged samples were tested over a range of temperatures from room temperature to 175^0 C, Figure 13. The hoop stress during RHGT of the 800 PPM sample was 90 MPa and resulted in no significant radial hydride formation.

Table 2 - Three Point Bend Test Sample Matrix				
	Hydrogen Level - PPM			
RGHT Hoop Stress - MPa	0	200	400	800
0	x			x

90				x
130		x		
170			x	

The 24^0 C load –deflection curves for as received, 200, 400 and 800 PPM samples are shown in Figure 14. The 200, 400 and 800 PPM samples had distinct failures with loss of load after about 10 mm, 8.3 mm and 6 mm deflections respectively at room temperature. The as-received tube sample accommodated a deflection of about 10 mm before experiencing a small load drop but not a brittle failure. This may be an effect of minor buckling in the ductile tube. For the as-received sample the total deflection at test end was about 13.3mm.

The axial bend results indicated that the high hydrogen – low radial hydride samples (800 PPM) had less ductility than the low hydrogen – high radial hydride samples (200 – 400 PPM). This trend is opposite to the trend seen in the RCT tests where the ductility is lower for the samples with high radial hydriding and lower hydrogen levels.

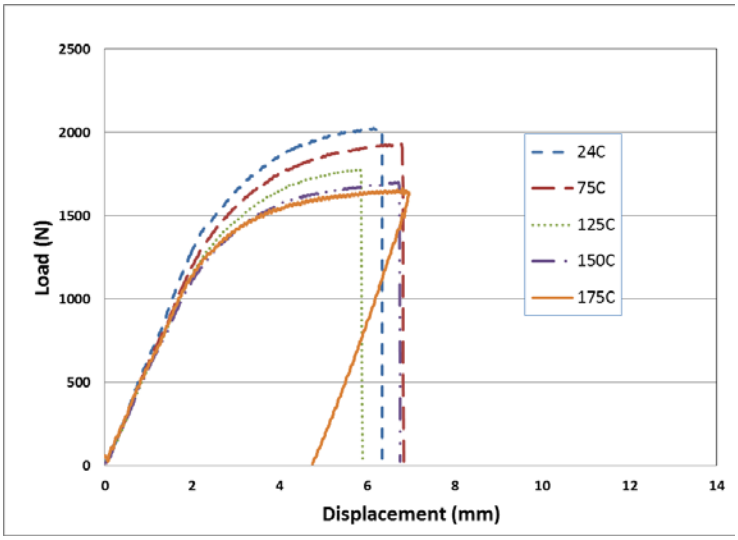

Figure 13- 800 PPM, 90 MPa RHGT, TPB Testing Results

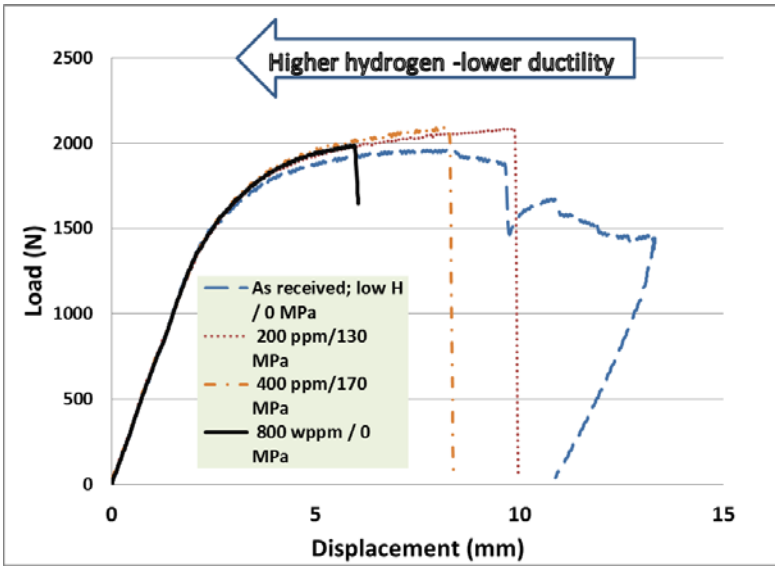

Figure 14 -Three Point Bend Test at 24C

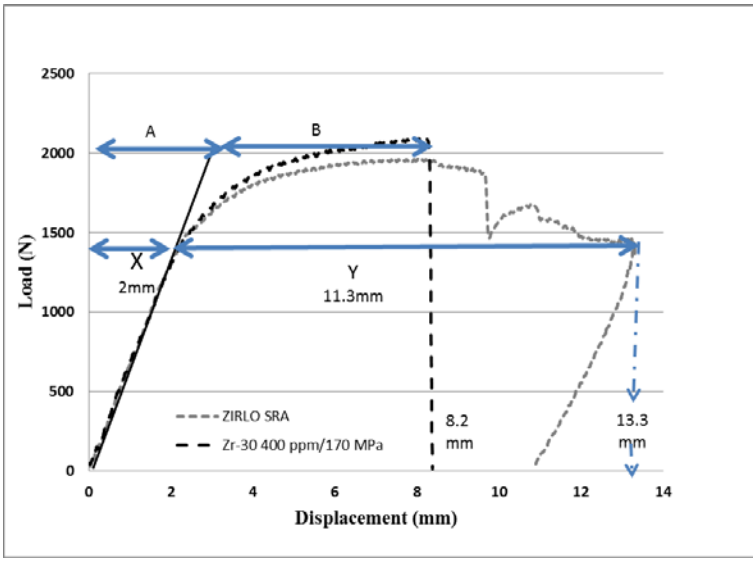

Figure 15 - Three Point Bend Test Relative Ductility Calculations

For the TPB test data it is difficult to characterize the DBTT characteristics without making some assumptions regarding relative ductility similar to those made for the RCT tests. For this set of TPB tests the deflection of the as-received sample is assumed as the base strain with no hydride effects. The initial TPB test results were characterized by comparing the plastic deflection of the as received tube (at reaching planned maximum test deflection) with the plastic deflection of the hydrided samples. An example of the value calculations is shown in Figure 15. For evaluating plastic deflection (Y) the elastic deflection is subtracted from the total deflection. As an example for the as-received sample this results in the calculated plastic base deflection of Y or 11.3 mm (13.3mm total – X (2 mm) elastic). The relative plastic strain values of the hydrided samples were calculated using the same technique. For example in Figure 15 the plastic

deflection (B) 5.1 mm for the hydrided sample Zr-30 is calculated by subtracting the elastic deflection (A) 3.1 mm from the total deflection of 8.2 mm.

The calculated plastic deflections from the TPB tests were normalized as a fraction of the plastic deflection of the as received and non-hydrided sample. The results are summarized in Figure 16. The results range from around 0.25 to 0.58 (25 % to 58 %) of the control sample. These are not real strains but are values that provide a relative comparison of ductility between the samples for the test parameters.

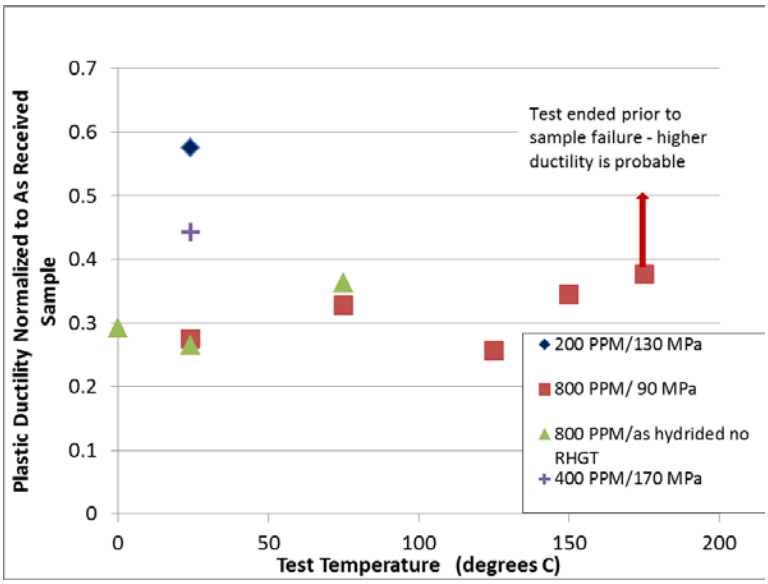

Figure 16 - Effects of temperature and Hydrides on Three Point bend Ductility

The number of TPB tests was limited in this program and the TPB-DBTT matrix was populated as shown in Table 3. For ease of comparison, the corresponding RCT- DBTT is shown in brackets. The 200 and 400 PPM TPB- DBTT values are estimates based on the results from test at RT where they were observed to have reasonable ductility and; thus, the DBTT was estimated to be lower than RT. The data does indicate a significant difference in DBTT depending on the failure mode. For the pinch /RCT failure mode the DBTT increases with lower hydrogen levels combined with hoop stress and a high radial hydride ratio. Material with high circumferential hydrides levels tends to have good – lower DBTT. The reverse is found for the axial bend / TPB test where high hydride levels even with no radial hydriding produces the highest estimated DBTT and samples with high radial hydride ratios have DBTT levels below room temperature. Thus when evaluating spent fuel performance for an axial bend condition the high hydrogen location will be critical while for a pinch load if there is a significant hoop stress present (radial hydriding) then the lower hydride area may be more critical regarding DBTT.

The comparisons of DBTT for RCT and TPB tests indicate that each test mode has a significantly different DBTT characteristic and response trend to hydride morphology variations. This is due to the crack initiation and propagation mode in the anisotropic crystal structure of

alpha zirconium combined with the hydride morphology and alignment with the crack plane and the reduction in low temperature ductility with large quantities of hydride formation. This

Table 3 – Three Point bend DBTT [*RCT- DBTT Values*]

	RGHT Nominal Pressure (MPA)			
RHGT Hydrogen Level (PPM)	0	90	130	170
0	<RT			
200			<RT [*75 C*]	
400				<RT [*110 C*]
800	<75 C [<*RT*]	~175 C [<*RT*]		

observation suggests that it is important to consider the specific failure mode when determining an applicable DBTT since RCT data does not represent axial bend characteristics. When evaluating the potential for pinch mode failure the effects of pellet resistance to large diameter deformations should be considered. Some points that suggest that a pinch failure is not very probable include:

- Assuming that there is at the time of fuel discharge a pellet clad diameter gap of 0.05mm (2 mils) total. These are liberal assumptions in that metallographic examinations of discharged fuel show no significant gap. However, the pellets are usually fractured and there is some equivalent gap associated with the cracks.

- The 0.05mm or 2 mil gap (without creep) restricts the clad displacement in a pinch mode or equivalent RCT test to only 0.05 mm prior to pellet contact at which time the load necessary for further displacement becomes significantly higher.

- As a worst case condition if during dry storage 1% creep occurs then there could be an additional gap of about 1mm. With current evaluations of temperature and hoop stress this is unlikely to occur but the result would be a diameter displacement of 0.15 mm prior to pellet contact which is still well below the 0.5mm displacement observed for clad failure in this test. Of course irradiated fuel clad will have different properties than the un-irradiated material tested here but it is proposed that the general trends of the hydride morphology versus RCT-DBTT and TPB-DBTT are still applicable.

- As an example, one of the most brittle RCT samples required 0.5mm diameter displacement prior to crack initiation. That failure point of an empty clad sample is a significantly higher displacement /strain than can be reached without encountering significant resistance from any pellet present in an actual fuel rod. This condition is shown graphically in Figure 17

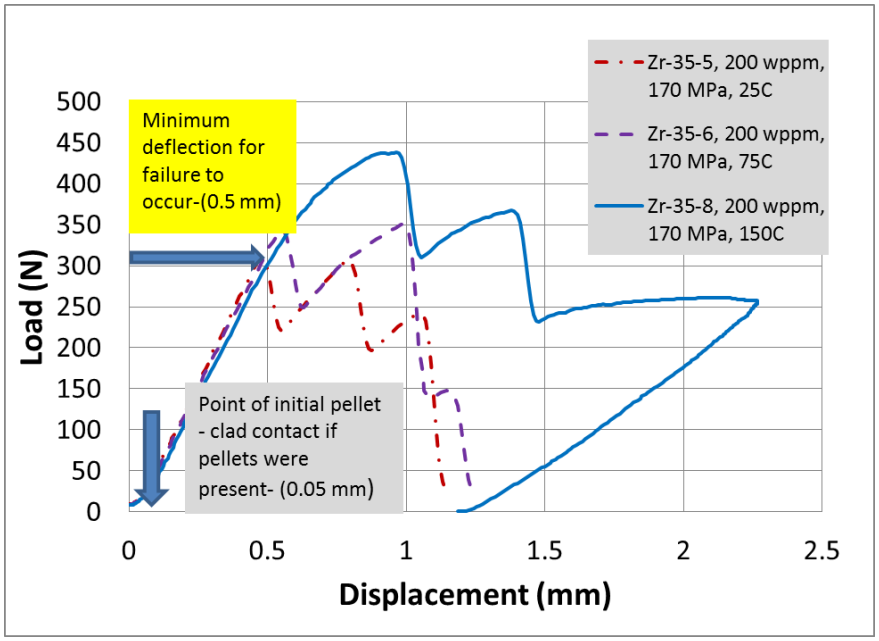

Figure 17 - Example of RCT test Showing Relative Displacements for Clad Contact with Pellet and Failure Deflections

- Even if the pellet crushes, granulates and flows like a liquid there is a resistance to further deformation based upon the reduction in fuel rod cross section related to the clad ovalization.

Hydride Morphology and Quantification

For this series of tests the technique of a grid overlay was used to provide comparable values of radial hydride orientation. The use of an overlay is a simple technique that can be easily adopted for use when the sample population is small. The number of circumferential hydrides intercepting the vertical grid lines is counted along with the number of radial hydride intercepts on the horizontal lines. A 45 ^{0} angle was used as a guideline to differentiate hydrides that intersect the lines at oblique angles. The data was evaluated looking at different hydride characteristics. For example, by counting the radial hydrides that have multiple grid intercepts, a value of "long" radial hydrides is obtained. By comparing the counts of radial and circumferential hydrides a relative ratio and the total radial and circumferential hydride count were obtained. Also information related to specific sections (ID, OD etc.) can be generated.

The evaluation included twelve hydrided and RHGT aged samples. They encompass a range in hydrogen levels of 100 to 800 PPM and RGHT stresses from 90 to 170 MPa. Figure 18 shows the relation of the radial hydride to circumferential hydride characteristic to the measured RCT DBTTs. There are multiple data points at the 24 ^{0}C – zero count position. The DBTT variation as a function of long hydrides was evaluated but does not provide a direct DBTT-to-hydride

length relationship for low long hydride densities and lower DBTT. The ratio of radial to circumferential hydrides shows good linear correlations with DBTT over the full DBTT range. Since the total radial hydrides can be more subjective and more affected by the sample preparation, the ratio parameter was preferred over an absolute hydride count. This evaluation supports the position that the ratio of radial hydrides in the clad is a critical factor in determining RCT-DBTT. Figure 18 also includes samples with the varying levels of hydrogen. While there is some scatter in the data points it is concluded that the radial hydride ratio and not the total hydrogen is the predominate factor in RCT DBTT characteristics. For axial bending DBTT the important factor is total hydrides and the ratio of radial hydrides is not a significant variable. This is similar to the conclusion regarding axial properties in reference **6.**

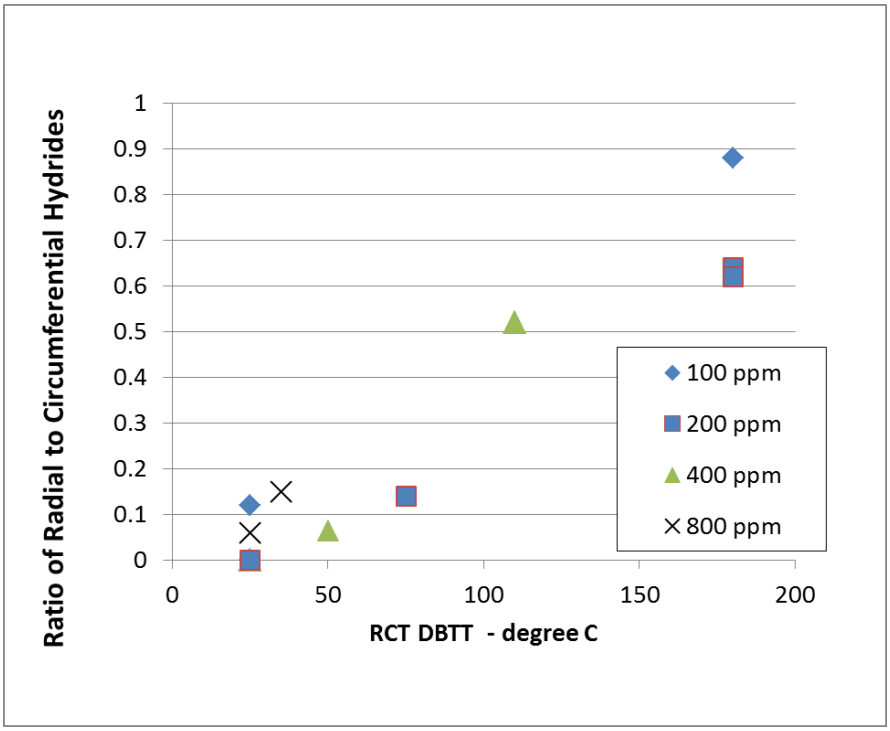

Figure 18 - The RCT- DBTT as a Function of the Radial Hydride Ratio

FEA Modeling

To better understand the stress and strain conditions and to expand them to potential accident conditions, finite element models were constructed to simulate the RCT and the three-point bend tests. The RCT model contained 16,000 eight-node three-dimensional reduced integration elements (Abaqus element type C3D8R) **[7]** with 18,954 nodes. Because of symmetry, only one-quarter of the ring is modeled. The full model rendition is shown in Figure 19, where the ring is loaded by a platen on the top, and the bottom plate is fixed in space. Frictionless contact is assumed in the analysis. The color (or grey scale) contours in Figure 19 are the von Mises stress distribution in MPa when the platen is displaced about 2.5 mm. The plot does not distinguish between tension and compression stresses.

Similarly, the finite element model for the three-point bend is shown in Figure 20. For clarity, the glass/quartz fillers used to simulate the fuel pellets are removed from the figure. The von Mises stress contours are those in the cladding only. The interaction between the fillers and the tube is modeled by frictionless contact. Only one-quarter of the model is needed for calculation. In this case the loading pin has been displaced about 9.1 mm while the support pins are fixed. The model uses 17,280 three-dimensional C3D8R elements with 20,979 nodes for the cladding (tube) and 1420 elements with 1827 nodes for the fillers.

In these exploratory calculations, the cladding material is assumed to be elastic-plastic and large deformation is permitted. The mechanical properties for Zircaloy-4 are chosen. The Young's modulus for the cladding is 9.3 GPa and the Poisson's ratio is 0.37 **[8]**; and the yield stress is 638 MPa, tensile strength (UTS, or the ultimate tensile strength) is 737 MPa (781 MPa in true stress), and the uniform elongation limit is 6% (5.8% in true strain) **[9].** Note that the vendor specifications **[8]** for the room temperature yield stresses are 381 (Longitudinal) and 467 MPa (Transverse); and the tensile strengths are 541 MPa (Longitudinal) and 514 MPa, (Transverse), but these anisotropic properties are not used in the current analysis. Linear elastic properties are assumed for the glass/quartz fillers in the three-point bend model with the Young's modulus 70,000 MPa and the Poisson's ratio 0.22.

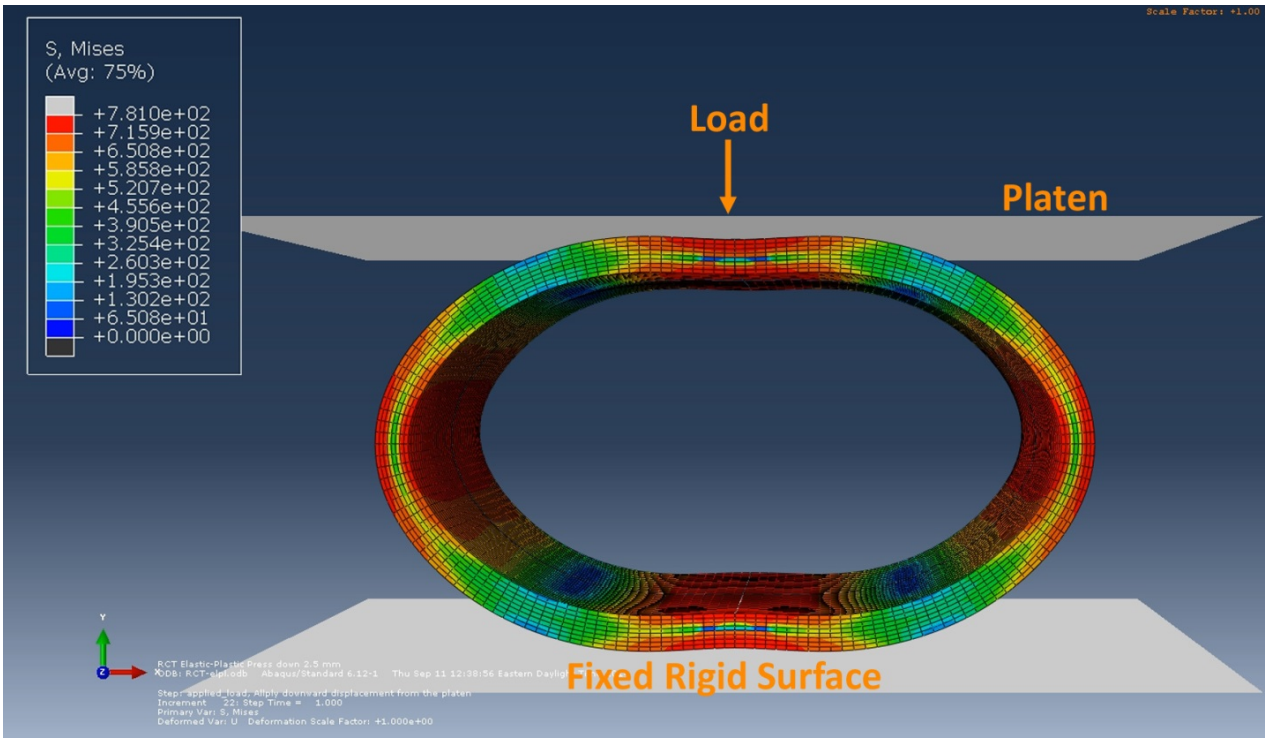

Figure 19 – An example of the finite element model for ring compression test

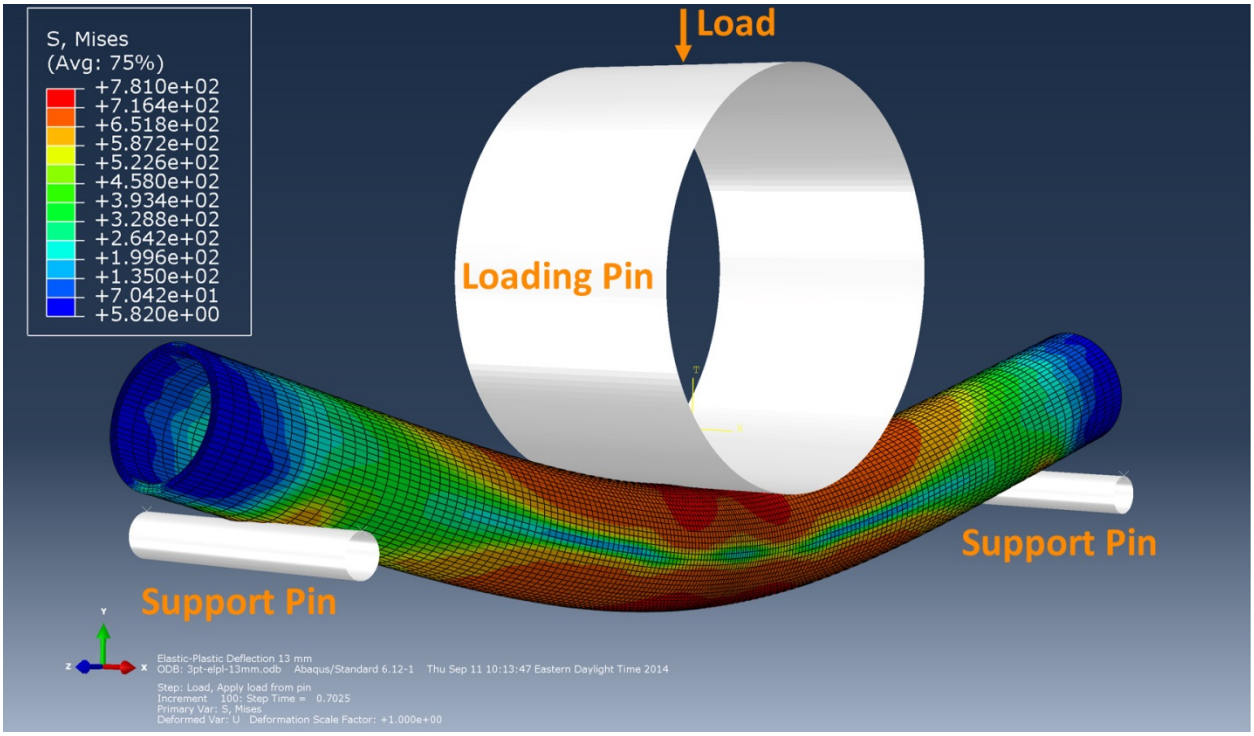

Figure 20- An example of the finite element model for three-point bend test

The experimental results indicate that the maximum hoop strains and stresses occurred at 12/6 and 3/9 o'clock directions of the specimen in RCT. The calculated maximum strains and stresses are shown in Figures 21 and 22. It appears that these maximum values are reached first in the 12/6 o'clock direction, that is, either under the load point (platen) or above the rigid support plate on the bottom in the inside diameter locations. In general, the present RCT finite element results are consistent with the RCT hoop stresses and strains calculated by Daum et al. [**9** and **10**], and are consistent with the RCT load- displacement test data reported by Billone et al. [**5**].

An offset strain (offset displacement normalized by the pre-test outside diameter of the ring) of 2% was defined by Billone **[5]** as the ductile-to-brittle transition strain for Zircaloy cladding materials. When the test ring exhibits greater than 50% wall cracking prior to reaching this transition offset strain (2%), the ring is considered brittle at the test temperature. In the present finite element model, the hoop strains are estimated between 0.3 to 0.5% (Fig. 21) at the ductile-to-brittle transition strain (2%); and the corresponding stresses are between 300 to 600 MPa (Fig. 22). The computational results also showed that the load-displacement response within this range is linear.

The maximum axial strain and stress of the three-point bend test are included in Figures 21 and 22. They are typically located on the outside diameter opposite to the load point where the maximum bending occurs. The calculation is stopped as the load point deflection approaches 9.1 mm for the glass/quartz filled tube model due to the limited ability to deform under the load point after the contact is made between the fillers and the tube wall. However, the hollow tube is able to deform up to 13 mm because of its flexibility. The true strain of the hollow tube is also included in Figure 21 for information.

The FEA analysis indicates that the stress levels differ between the ID and OD of the RCT sample and differences would exist in the TPB IDs and ODs. As discussed the RCT and TPB ductilities are consistent within the 800 PPM data sets and suggest that the ID-OD rim position is not a large variable and does not significantly impact the trend comparisons between the 800 PPM samples and the 100, 200, and 400 PPM samples.

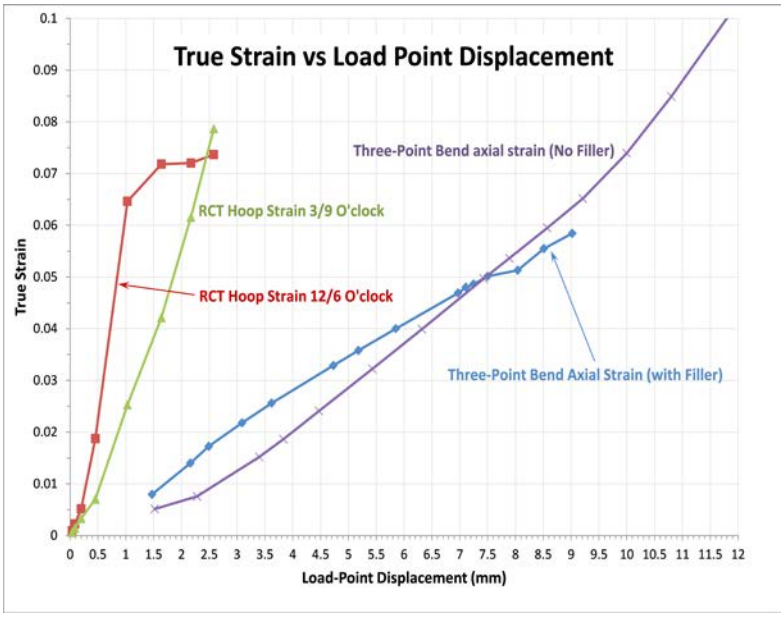

Figure 21- Maximum strains for the ring compression test and the three-point bend test

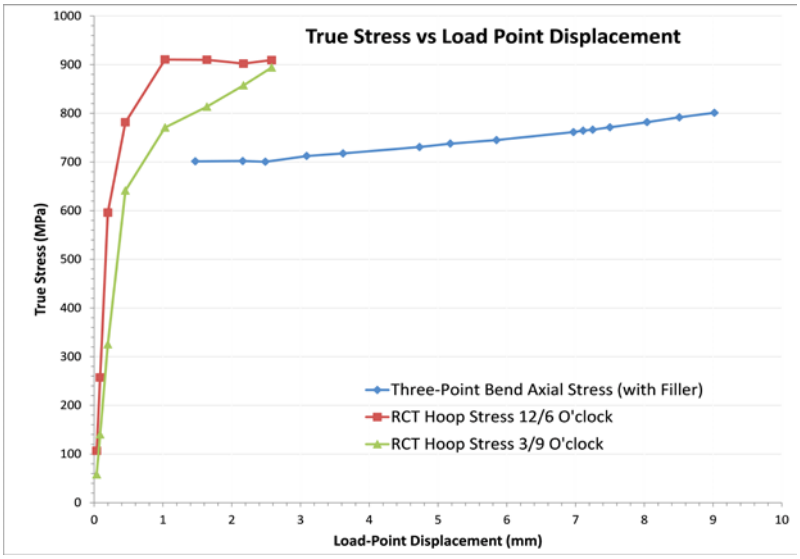

Figure 22- Maximum stresses for the ring compression test and the three-point bend test

Based on the evaluation of FEA results for filled and non-filled tubes, it can be concluded that the function of the fillers is to maintain the cross-section (when the fillers are intact), and to

effectively transfer the intended deformation to the tensile part of the tube (as the three-point bend of a solid beam). The FEA results of a hollow pipe shows that, at the same loading pin displacement, the maximum axial strain (E33) on the outer fiber is higher when the fillers are present. Without the fillers, significant energy is used for wide-spread plastic deformation (e.g., to crush the hollow pipe). On the opposite, the maximum axial stress (S33) is higher in the case of the non-filled pipe. Note that the location of the maximum E33 may not coincide with the location of the maximum S33. It is not easy to explain the stress component because it is computed from the strain tensors (6 independent components for isotropic materials) and it gets more complicated in elastic-plastic calculations (nonlinear stress-strain curve and finite strains in large deformation). On the other hand, the strains are easier to visualize because it is based on the displacement vector (3 independent components). With the strain (E33) results, it may be able to explain the experimental claim why the buckling or crinkle occurred before the cracking/failure took place when fillers were not inserted.

FEA key observations

A) At the initial displacement (0 to 1mm) of the RCT test the stress and strains increase. After this displacement there is a plastic displacement at the N-S (6/12 O'Clock) position where the clad deforms to the loading platens and the stress-strain is distributed over a larger surface and the peak stress and strain do not significantly increase with additional displacement.

B) At the initial displacement of the RCT tests the stress and strain at the N-S (6/12 O'Clock) positions (clad ID) are significantly greater by a factor of 3 to 4 relative to the E-W (3/9 O'Clock) positions (clad OD). However the E-W (3/9 O'Clock) position does not distribute the load in the same fashion and the N-S (6/12 O'Clock) position and after about 2.4 mm displacement the two positions are at about equal peak stress and strain. With further displacement the E-W (3/9 O'Clock) (clad OD) position becomes the peak stress-strain location. This evolution is important to consider when evaluating RCT results. For example, the impacts of ID surface condition, OD hydride rims and hydride morphology on crack initiation.

C) The TPB requires significantly greater deflections compared to the RCT to achieve similar material yielding. A general comparison between failure points for RCT and TPB samples shows similar true strain levels at failure. The more brittle RCT failures occurred at about 0.6 – 0.75 mm displacement. The FEA indicates that the peak true strains at these deflections are about 0.03 to 0.05 mm/mm. These equivalent peak FEA strains for the TPB test are associated with deflections in the range of 4.5 to 7 mm. At about 6 mm the brittle failure of a 800 PPM sample was observed indicating a degree of equivalency in the failure strains between the RCT and TPB tests.

Quartz Pellet Testing Characterization tests

For background information regarding the impacts of pellets on the clad deformation during a pinch loading some RCT tests were performed on samples containing a quartz pellet as used in the TPB tests. There were two types of compression testing. One test series was on a bare pellets and another on a clad sample with a pellet on the inside. The pellet ends were not restrained. The load displacement curves are found in Figure 23 and show that for the bare sample a load of about 9000 N is withstood before quartz pellet failure. With the quartz in the clad there is a displacement of about 0.38 mm before clad-pellet contact after which the load to failure goes to about 14000 N. The failure resistance of the quartz-clad system is higher than just the bare quartz and the displacement resistance with the quartz pellet in place is 20 times the displacement load at which a bare clad sample fails. While quartz pellets do not replicate actual burned fuel pellet conditions, the observations supports the assumption that pinch failures of loaded fuel rods will be significantly different than those parameters observed in the RCT testing of empty tubes. Even though the pellets are fractured during reactor operation they still will provide significant support against clad diameter deflection. This is not a new observation and has been studied in the past, Reference **11** is an example.

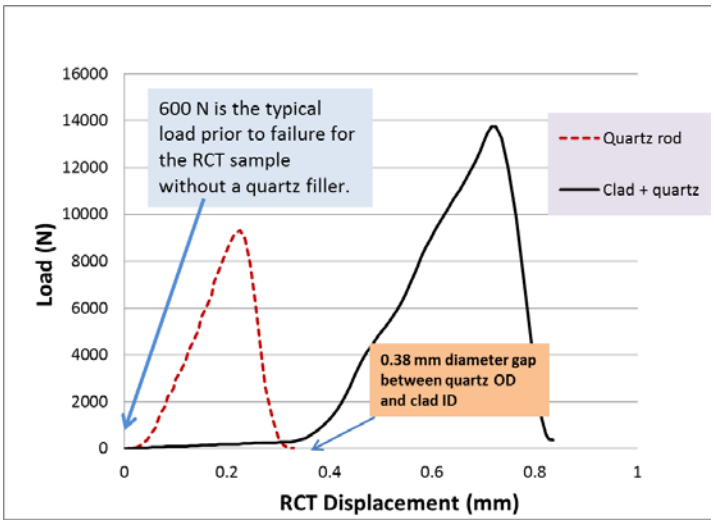

Figure 23 - Compression Tests on Quartz Filler

Conclusions

From the RCT -DBTT results it can be conclude that for the conditions tested:

A. There was no significant radial hydride re-orientation with the 90 MPa RHGT. The resultant DBTT for the unirradiated samples with 100 to 800 PPM is lower than RT.

B. When radial hydrides are present there is a significant effect on RCT related DBTT. For example with a 170 MPa RGHT the RCT-DBTT is about 180^0 C for 200 PPM hydrogen. This

strong impact of radial hydrides on RCT DBTT is postulated to be associated the RCT crack propagation being parallel to the radial hydride planes.

C. The RCT sample with lower hydrogen levels (100 – 200 PPM) shows more sensitivity to the RHGT stress than the samples with high hydrogen content. The DBTT levels for equivalent RGHT hoop stresses are higher for the lower hydrogen containing samples (100 – 200 PPM) relative to the 800 PPM samples. The difference is attributed to radial to circumferential ydride ratio in the microstructure.

D. The FEA –RCT results are consistent with general knowledge in that there is a difference in the stress and strain generation rates versus diameter displacement for the four prime directions and that the ID surface in the N-S direction experiences the highest strain initially and that the OD surface in the E-W direction experiences a slower rate of strain increase than the N-S position but eventually exceeds the N-S peak strain at high displacements..

From the TPB tests -DBTT results it can be conclude that for the conditions tested:

A. The DBTT generated using RCT does not represent the DBTT characteristic of axial bend – TPB tests. In evaluating spent fuel performance under accident conditions it is critical to use properties representative of the specific failure mode.

B. High hydrogen levels rather than high radial hydrides are detrimental to TPB DBTT. This effect is postulated to be at least partially due to the relative direction of the TPB crack propagation relative to the circumferential and radial crack orientations.

C. The FEA-TPB results regarding failure strains are consistent with failure strains observed in the FEA results from the RCT tests.

D. Axial bending failure modes are postulated to be more probable than diameter pinching. Likewise, radial hydriding is not a significant factor in axial bend DBTT and thus the concern regarding the degree radial hydriding may not be as critical to performance as initially considered.

REFERENCES

[1] P. Korinko. R. Sindelar, and R.Kesterson “Comparison of Ring Compression Testing to Three Point Bend Testing for Unirradiated ZIRLO Cladding,”, Proceedings of the ASME 2015 Pressure Vessel and Piping Conference, Paper No. PVP2015-45984, July 19-23, 2015 Boston Massachusetts, USA; ISBN: 978-0-7918-5702-1; pp. V007T07A055; 10 pages
[2] NRC Spent Fuel Project Office Interim Staff Guidance - 11, Revision 3, http://www.nrc.gov/reading-rm.html
[3] T. L. Sanders, K. D. Seager, Y. R. Rashid, et al “A Method for Determining the Spent-Fuel Contribution to Transport Cask Containment Requirements,” SANDIA Report, SAND90- 2406, TTC-1019, UC-820, November 1992.

[4] Gregg A. Morgan, Jr, and Paul S. Korinko, "The Adsorption of Hydrogen on Low Pressure Hydride Materials" Conference Proceedings, Material Science and Technology 2011, October 16-20, 2011, Columbus, OH
[5] Billone, M. C., Burtseva, T. A., and Einziger, R. E, "Ductile-to-brittle transition temperature for high-burnup cladding alloys exposed to simulated drying-storage conditions," Journal of Nuclear Materials, 433, pp. 431-448, 2013.

[6] Chu, H.C., Wu, S.K., Chien, K. F., and Kuo, R.C. "Effect of radial hydrides on the axial and hoop mechanical properties of Zircaloy-4 cladding," Journal of Nuclear Materials, 362 , pp. 93-103, 2007
[7] Abaqus Version 6.12-1, Dassault Systemes Simulia Corp., Providence, RI, USA
[8] ATI Wah Chang Zirconium Alloy Zircaloy-4: http://www.matweb.com/search/datasheettext.aspx?matguid=a265da2e4ff94c968a8ae344870a32e3
[9] Daum, R. S., Majumdar, S., Tsai, H., Bray, T. S., Koss, D. A., Motta, A. T., and Billone, M. C., "Mechanical Property Testing of Irradiated Zircaloy Cladding Under Reactor Transient Conditions," Small Specimen Test Techniques: Fourth Volume, ASTM STP 1418, M. A. Sokolov, J. D. Landes, and G. E. Lucas, Eds., ASTM International, West Conshohocken, PA, 2002.
[10] Daum, R. S., Majumdar, S., Liu, Y., and Billone, M. C "Radial-hydride Embrittlement of High-burnup Zircaloy-4 Fuel Cladding," Journal of Nuclear Science and Technology, 43:9, pp. 1054-1067, 2006.
[11] Y. Rashid,"Spent Fuel Transportation Applications-Assessment of Cladding Performance," EPRI Report 1015048, December 2007.